



HAL
open science

Very low resistance Al/Cu joints for use at cryogenic temperatures

Sébastien Triqueneaux, James Butterworth, Johannes Goupy, Clément Ribas,
David Schmoranzer, Eddy Collin, Andrew D Fefferman

► **To cite this version:**

Sébastien Triqueneaux, James Butterworth, Johannes Goupy, Clément Ribas, David Schmoranzer, et al.. Very low resistance Al/Cu joints for use at cryogenic temperatures. *Journal of Low Temperature Physics*, 2021, 203 (3-4), pp.345-361. 10.1007/s10909-021-02575-x . hal-02931574

HAL Id: hal-02931574

<https://hal.science/hal-02931574>

Submitted on 11 Jul 2023

HAL is a multi-disciplinary open access archive for the deposit and dissemination of scientific research documents, whether they are published or not. The documents may come from teaching and research institutions in France or abroad, or from public or private research centers.

L'archive ouverte pluridisciplinaire **HAL**, est destinée au dépôt et à la diffusion de documents scientifiques de niveau recherche, publiés ou non, émanant des établissements d'enseignement et de recherche français ou étrangers, des laboratoires publics ou privés.

Very low resistance Al/Cu joints for use at cryogenic temperatures

Sébastien Triqueneaux · James Butterworth · Johannes Goupy · Clément Ribas · David Schmoranzer · Eddy Collin · Andrew Fefferman

Received: date / Accepted: date

Abstract We present two different techniques for achieving low resistance (<20 n Ω) contacts between copper and aluminium at cryogenic temperatures. The best method is based on gold plating of the surfaces in an e-beam evaporator immediately after Ar plasma etching in the same apparatus, yielding resistances as low as 3 n Ω that are stable over time. The second approach involves inserting indium in the Al/Cu joint. For both methods, we believe key elements are surface polishing, total removal of the aluminum oxide surface layer, and temporary application of large (typ. 11 kN) compression forces. Such contacts are not demountable. We believe the values for gold plated contacts are the lowest ever reported for a Cu/Al joint of a few cm². This technology could simplify the construction of thermal links for advanced cryogenics applications, in particular that of extremely low resistance heat switches for nuclear demagnetization refrigerators.

Keywords Sub-Kelvin · Contact resistance · Heat switches · Nuclear demagnetization refrigerators

1 Introduction

Dry dilution refrigerators have widely spread in laboratories these last years, opening the mK temperature range to a large community. Yet, some research fields still require lower temperatures. As an illustration, a European project has recently been granted [1] aiming at providing access to platforms in the

S. Triqueneaux · J. Goupy · C. Ribas · E. Collin · A. Fefferman
Univ. Grenoble Alpes, CNRS, Grenoble INP, Institut Néel, 38000 Grenoble, France
E-mail: sebastien.triqueneaux@neel.cnrs.fr

J. Butterworth
Air Liquide Advanced Technologies 2, rue de Clémencière, BP 15, 38360 Sassenage, France

D. Schmoranzer
Charles University, Ke Karlovu 3, 121 16, Prague, Czech Republic

micro-kelvin range. Nuclear demagnetization refrigerators (NDRs) pre-cooled by dry dilution fridges seem a straightforward extension of the temperature range below 1 mK. Successful developments [2,3] either with Cu or with PrNi₅ as nuclear coolant have validated this concept.

NDRs are not intrinsically continuous coolers as they need to be recycled. In wet dilution refrigerators, i.e. those using liquid helium as a 4.2 K precooling source, nuclear stages can remain at base temperature typically for a couple of days or, in some cases, for up to a month (see [4] and references therein). In these examples, the heat leak is typically well below 1 nW. In dry fridges, the induced vibrations associated with pulse-tube coolers [5,6] can lead to a significant heat input and values of the order of 5 nW have been reported [2, 3]. For a given setup, this will shorten the experimental time at base temperature. For this main reason, but also since operation in the sub-mK regime for months would be of interest for some experiments, there is a need for the development of a continuous nuclear demagnetization refrigerator (CNDR) as already proposed by Toda et al. [7].

In a previous paper [8], we have presented a CNDR concept based on two PrNi₅ nuclear demagnetization stages (NDSs) mounted in series (see Fig. 1) and separated by a heat switch. This architecture, aimed at providing continuous operation below 1 mK, is similar to the one used for electronic adiabatic demagnetization refrigerators for space applications [9]. According to our simulations [8], the thermal link between the 2 stages is the most critical point: its thermal resistance must be minimized. This is detailed in the following section.

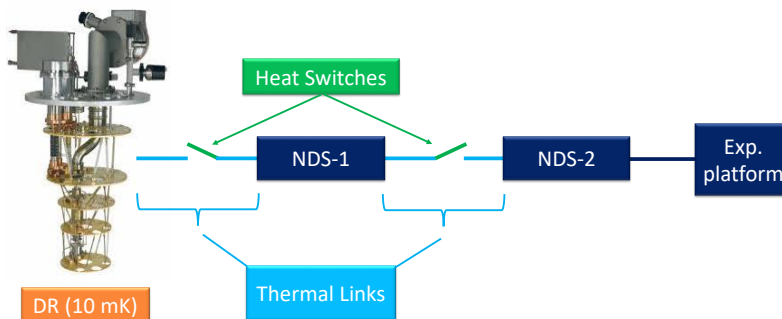


Fig. 1 Overview of the Continuous Nuclear Demagnetisation Refrigerator (CNDR). DR stands for Dilution Refrigerator and NDS stands for Nuclear Demagnetisation Stage. Note that, for clarity, the coils around the NDSs and the superconducting heat switches are not represented.

In a more recent paper [10], we have compared parallel and series configurations. Although the parallel configuration may provide better performance and relax the constraint on the thermal link resistance, it requires more space and is more complex since it requires 4 heat switches instead of 2. Whichever the selected configuration, the thermal link resistance should be minimized.

In the present work, we report stable Al/Cu contact resistances as small as $3 \text{ n}\Omega$. This achievement may allow construction of superconducting heat switches with a normal state resistance $\leq 15 \text{ n}\Omega$, which is the lowest value reported so far [11]. Furthermore, the construction of our gold-plated Al/Cu joints rely on removal of the aluminum oxide layer by plasma etching and subsequent gold deposition without breaking vacuum. Our process avoids the complicated and potentially dangerous cyanide-based chemistry employed in [11].

2 Thermal link issue

Fig. 2 highlights the criticality of the thermal link between NDS1 and NDS2. According to the model developed in [8,10] and assuming a minimum field-independent heat leak of 5 nW , it is not possible to maintain a base temperature below 1 mK for a thermal link resistance of $500 \text{ n}\Omega$. With $150 \text{ n}\Omega$, the model suggests that the base temperature could be as low as $750 \text{ }\mu\text{K}$ for 10 nW losses. It is expected that this provides sufficient margin to allow for uncertainties inherent to the model. As a consequence, this value of $150 \text{ n}\Omega$ can be considered an appropriate objective value.

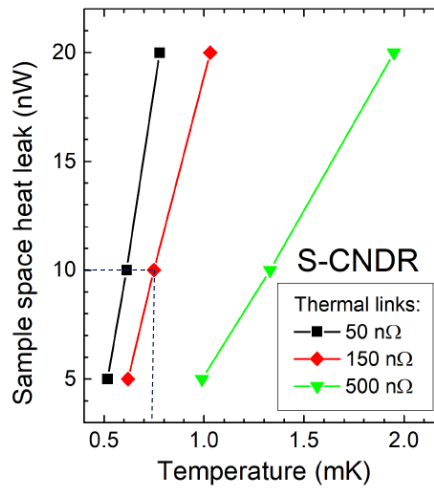


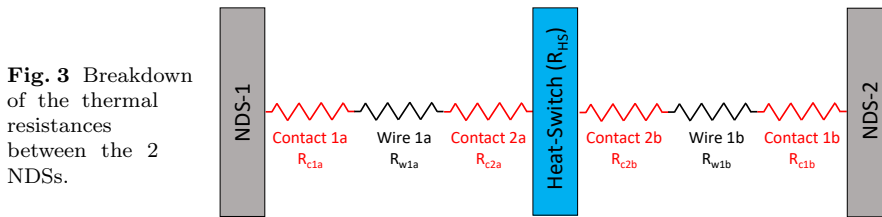
Fig. 2 Final temperature (x) for different heat leaks (y) and different values of the NDS1-NDS2 thermal link electrical resistance (heat switch in its normal state) taken from [8]. Dashed lines identify the selected parameters.

In the following, we have used the Wiedemann-Franz law to convert thermal resistances into electrical resistances. As an example, an electrical resistance of $150 \text{ n}\Omega$ corresponds to a thermal resistance of $\approx 6000 \text{ K/W}$ at 1 mK which would lead to an acceptable ΔT of $60 \text{ }\mu\text{K}$ between the 2 NDS for 10 nW applied power. Although this law can overestimate the thermal conductivity [9, 12] for some materials or for contact resistances, we assume it is satisfactory for comparison purposes.

In order to evaluate whether this requirement was achievable, we have reviewed some of the articles dealing with superconducting heat switches for NDRs. Results are summarized in Table 1. The equivalent electrical resistances vary over almost 4 orders of magnitude, but at least 6 systems exhibit values close to or below $100 \text{ n}\Omega$ and the lowest reported value is only $15 \text{ n}\Omega$. This suggests that our goal value of $150 \text{ n}\Omega$ for the entire thermal link between the 2 NDSs might be achievable.

3 Thermal contact issue

Fig. 3 provides a breakdown of the contributors to the thermal link resistance between the 2 NDSs.



For the determination of the electrical resistances, we have used the following assumptions:

- Wires 1_a (wires 1_b are considered identical): 6 copper wires of 6N purity [37], 1.5 mm diameter and 5 cm long. RRRs above 5 000 have been achieved several times on wires from the same batch after heat treatment. This results in $16 \text{ n}\Omega$ per set of wires, so $32 \text{ n}\Omega$ total contribution for R_{w1a} and R_{w1b} .
- The Heat-Switch will be made of Aluminium. Although its geometry is not fixed yet, it could be a C-shape block as already used at Lancaster (see [14] for example) with a section of $15 \text{ mm} \times 5 \text{ mm}$ and a thermal path

Table 1 A review of heat switches thermal performance (sorted by publication date).

Ref.	Mat.	Technology	Variable	Published Value	Equiv. R	Comments
[13]	Zn	Zinc foils soldered to copper	Thermal R.	$120/T \text{ K}^2\text{W}^{-1}$	$\approx 2900 \text{ n}\Omega$	
[11]	Al	Al foils pressed against copper foils + gold plating (zincate solution for Al)	Conductance	At 30 mK: $10 \mu\text{W}$ with a ΔT of 0.2 mK	15 n Ω	For the overall heat switch
[14]	Al	Bulk Al with silver wires - fusion under pressure	Electrical R.	$0.5 \mu\Omega$ per contact	$\approx 250 \text{ n}\Omega$	For 4 contacts in parallel and 2 in series and negligible contribution of Al or Ag wires
[15]	Sn	Sn Switch	Conductance	$5 \times 10^{-3} T \text{ WK}^{-2}$	1200 n Ω	
[15]	In	In Test switch	Conductance	$0.4 T \text{ WK}^{-2}$	61 n Ω	
[16]	Al	Overall link between DR and 1 st NDS	Conductance	$0.24 T \text{ WK}^{-1}$	102 n Ω	
[16]	Zn	Five Zn foils (0.1 mm thick) pressed into Cu slits	Electrical R.	$0.4 \mu\Omega$	400 n Ω	Measured at 4.2 K
[16]	Zn	Same as above	Conductance	$0.04 T \text{ WK}^{-1}$	610 n Ω	Between 12 and 35 mK
[16]	Al	Five Al foils (0.1 mm thick) pressed into Cu slits + tungsten washers	Electrical R.	$0.1 \mu\Omega$	100 n Ω	
[16]	Al	Same as above	Conductance	$0.2 T \text{ WK}^{-1}$	122 n Ω	Between 1.1 and 3.8 mK
[16]	Pb	$10 \text{ mm} \times 20 \text{ mm} \times 1 \text{ mm}$ bolted to Cu and Ag. Overall thermal link characterised	Electrical R.	$0.8 \mu\Omega$	800 n Ω	
[16]	Pb	Same as above	Conductance	$0.04 T \text{ WK}^{-1}$	610 n Ω	Between 18 and 35 mK
[16]	Pb	$10 \text{ mm} \times 20 \text{ mm} \times 1 \text{ mm}$ bolted to Cu and Ag. Shorter Ag foils. Overall thermal link characterised	Electrical R.	$0.2 \mu\Omega$	200 n Ω	
[16]	Pb	Same as above. Degradation with time	Conductance	$0.03 T \text{ WK}^{-1}$	813 n Ω	Between 4 and 10 mK. Degradation after a few cool down
[17]	Al	3 Al foils (0.4 mm thick) diffusion welded to 4 Cu foils (0.2 mm thick)	Electrical R.	400 n Ω	400 n Ω	
[18]	In	Rolled In wire soldered at each end	Conductance	$2.7 \times 10^{-4} T \text{ WK}^{-1}$	$\approx 90000 \text{ n}\Omega$	
[19]	Al	Eight 0.25 mm thick aluminium foils diffusion welded into Cu blocks	Electrical R.	100 n Ω	100 n Ω	
[20]	Zn	0.25 mm Zn foil diffusion welded to 0.5 mm Cu foils + pressed contacts to Cu blocks	Electrical R.	50 n Ω	50 n Ω	
[20]	Zn	Complete heat switch	Electrical R.	100 n Ω	100 n Ω	
[2]	Al	Seven banded aluminium foils ($50 \text{ mm} \times 10 \text{ mm} \times 0.5 \text{ mm}$ each) diffusion welded to two copper rods	Electrical R.	$2.4 \mu\Omega$	2400 n Ω	

length of approximately 35 mm. We have measured a RRR of ≈ 5000 with 6N purity [38] as received. The calculated contribution is $\approx 2 \text{ n}\Omega$.

As a result, and after applying a factor of 2 as a safety margin on the contributions of the Cu wires and Al heat switch, we end up with a budget of $\approx 20 \text{ n}\Omega$ for each of the 4 contact resistances. Once again the question arises whether such a value is achievable. We have first focused our efforts on the Al/Cu contact resistances (R_{c2a} and R_{c2b} in Fig. 3) leaving the PrNi₅-Cu contact for a future step.

Numerous articles provide data on contact resistances between metals (see for instance [21, 22, 23, 24, 25, 26]). We limit ourselves to the value of electrical resistance at low temperatures and do not consider their – sometimes non-linear – temperature dependence, which is addressed in [26]. We may identify 2 major trends in these data. A general trend is well represented in Fig. 4 taken from Blondelle et al. [21] and dealing with bolted Cu-Cu joints at 4.2 K. First, the resistances follow a $1/F$ dependence, where F is the applied Force, in agreement with theoretical predictions [26]. Furthermore, except for the measurements of Okamoto et al. (see below), values in the range of 100-400 n Ω are encountered for forces of 3000 N, close to the recommended force for standard M4 stainless steel bolts [21].

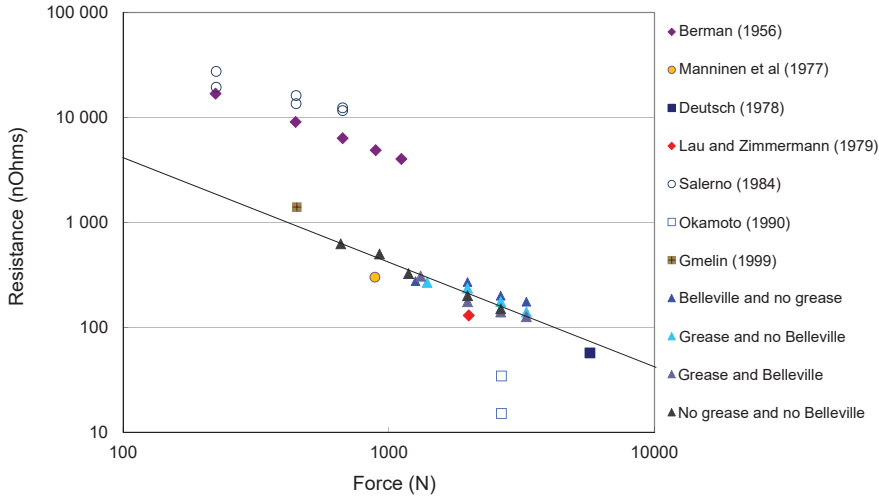


Fig. 4 Collection of experimental data for Cu-Cu contact resistances as function of applied force (from[21]).

This is consistent with the "conservative" approximation proposed in [22] for the thermal conductance of Cu-Cu bolted joints based on several earlier publications: $G = 0.0624 \times T - 0.00023$ [WK^{-1}]¹. This translates into a contact resistance R_c of ≈ 400 n Ω using the Wiedemann-Franz law, which is comparable to the figure given above. Similar values are also found in [24] where Salerno and Kittel report thermal conductances for Cu assemblies (not only Cu-Cu) ranging from 10^{-3} to $\approx 10^{-1}$ WK^{-1} at 4.2 K for 670 N applied force. With a linear dependence of the conductance with the applied force, then the best values at 3 kN would be close to 200 n Ω , again comparable to the figure given above.

Yet, a few authors report significantly lower values with different preparation techniques (we provide a detailed table in Appendix):

- Deutsch [27] achieved 77 n Ω by simply pressing copper samples one against the other.
- Mueller et al. [11] and Shigematsu et al. [28] for Al-Cu contacts used rather complex procedures making use of a Zincate solution followed by cyanide-based gold plating. They achieved 5 n Ω in the best conditions.
- Okamoto et al. [29] used non cyanide gold plating solutions. Their best results – 4 n Ω – were obtained adding an indium filler.
- Willekers et al. [30] used impact welding and achieved 32 n Ω .

Even if these measurements may appear exceptional compared to the large number of contact resistances above 100 n Ω , they suggest that a R_c of 20 n Ω for our Al/Cu contacts should be feasible.

Bad contact resistances with Al on one or 2 sides are often explained by the presence of a few nm Al_2O_3 hard film on the surface of aluminium. Such a hard oxide layer is difficult to get rid of and is detrimental for thermal contacts at very low temperatures. In the worst cases, the conductance of the contact would depart from the T dependence expected for metallic contacts [26]. Several ways are proposed to remove or disrupt this oxide layer:

- Wanner [31] reports Al to Al contacts with an equivalent electrical resistance of 70 n Ω for rough samples whereas polished samples give about 3 times this value. He suggests that the roughness combined with strong compression forces makes it possible to break the Al_2O_3 layer. The $R_c = 70$ n Ω was obtained for a large torque of 20 Nm onto a M8 screw. This R_c is too high for our application and applying such a torque is out of range for our future system (we will use M4 screws at best).
- We have performed tests using magnetic pulse welding inspired by developments in another field [32] but the results were not satisfactory.
- Impact welding, as successfully achieved by Willekers et al. [30] could be a promising approach, however it is unclear what effect this process might have on the highly annealed copper and aluminium required for our application.

¹ It seems surprising that, in this article from Schmitt et al., the conductance would not depend on the applied force. We suppose that this approximation is valid for their conditions, i.e. 3 kN.

- It is often proposed to chemically remove the oxide layer and replace it by a coating (usually gold). The results are sometimes clearly unsatisfactory when the process is not appropriate [31] but some very good results have been obtained as in [11,28]. In the chemical oxide removal, a zincate solution replaces Al_2O_3 with Zn or Cu and the Al sample can be exposed to air. It is then gold plated in a separate solution.
- An alternative solution proposed by Shigematsu et al. [28] drew our attention. It consists in using equipment dedicated to micro-electronics in order to sputter Au onto Al immediately after etching while remaining under vacuum. Despite their pessimistic conclusion on this approach, we have decided to investigate that process since we had already succeeded in removing the oxide layers on Al for other applications [33]. We have also decided to test Cu-Al connections with indium as a filler.

For clarity, we first focus on our successful procedures and results, i.e. our last runs. Our earlier trial-and-error tests that may provide some useful information are reported in subsequent sections.

4 Experimental setup

The experimental setup for the samples to be tested is depicted in Fig. 5 and 6. Small rectangular Cu pieces ($20\text{ mm} \times 12\text{ mm} \times 2.5\text{ mm}$) are pressed onto the 2 ends of a bigger Al block ($600\text{ mm} \times 20\text{ mm} \times 9.7\text{ mm}$) via 2 SS bars and 2×2 M6 SS screws + Belleville washers ($\varnothing_i = 6\text{ mm}$, $\varnothing_e = 12.5\text{ mm}$, $t = 0.7\text{ mm}$, max. deflection 0.4 mm). Smaller screws are screwed into the different materials for current supply or voltage measurement.

In order to establish a reproducible and well controlled tightening procedure, we made some preliminary tests. First, we pressed representative Cu pieces against an Al block at different torques. For each test, we would put a pressure measurement film (Fuji Prescale MS) between the two materials. Although the film does not give very quantitative results, it helped us fix 5 Nm as a minimum torque and underlined the need for alternative tightening of the screws in order to get a significant and homogeneous contact surface. It also confirmed that our polishing procedure (see below) would give a good planarity.

Then, we tested and characterised several Belleville washer configurations. Belleville washers are needed to ensure that the applied force remains constant while the setup is being cooled down – about $10\text{ }\mu\text{m}$ differential thermal contraction was expected for our device. The characterisation of the Belleville washers was judged necessary firstly because we could find very few technical data on compression characteristics of standard washers. We applied pressure on the screw head with a hydraulic press and measured the deflection of the washer assembly. The maximum measured stroke was $\approx 0.9\text{ mm}$, close to the expected 0.8 mm . We could verify that the deflection increases linearly with the applied force. For our setup, the slope would be 0.23 mm.kN^{-1} up to 3.5 kN . With this “calibration”, we could evaluate the force on our setup by measuring

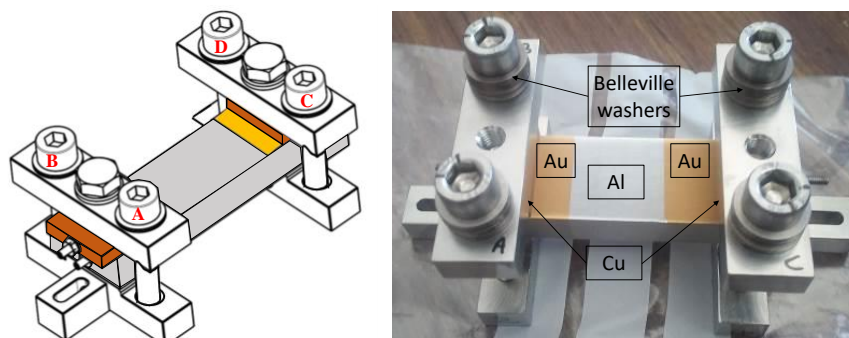
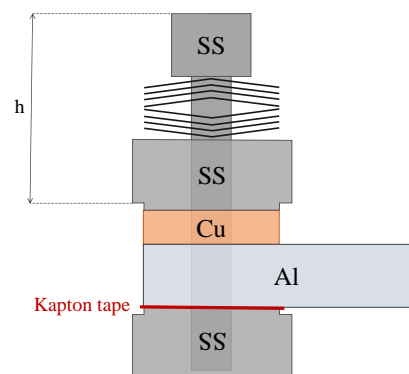


Fig. 5 Setup for resistivity measurements. Left: schematic drawing (Al in grey, Cu in orange, Au in yellow and SS in white). Right: assembly with an Al sample gold plated at the 2 ends. Note that Cu is not visible on the photo. Overall dimensions: $\approx 100 \text{ mm} \times 50 \text{ mm} \times 50 \text{ mm}$.

Fig. 6 Sectional view of one Cu-Al assembly with the 4 + 4 Belleville washer configuration used for our measurements. The height "h" is used to determine the applied force. Kapton tape is inserted between the lower SS bar and the Al block in order to get a negligible current flow through the SS screw – SS lower bar – Al block path.



the deflection ("h" in Fig. 6) instead of the torque applied on the M6 screws. This is far more reliable since, as detailed in Appendix, one cannot reliably convert a torque into a force. This latter observation was confirmed as we used different levels of cleaning for our M6 screws: similar applied torques would not compress the washers equivalently. This is explained by the variation of the SS-SS friction coefficient as a function of lubrication.

After assembly, the overall setup is mounted in a LHe cryostat.

5 Samples preparation

We have used the following bulk materials which were not heat treated for our tests:

- Al plate ($9.7 \text{ mm} \times 130 \text{ mm} \times 370 \text{ mm}$) - purity 4N6 [39]. On a test sample, we measured a RRR of ≈ 350 for the raw material.
- Standard CuC2 (\simeq OFHC) block. On a test sample, we measured a RRR of ≈ 130 for the raw material.

2 Al (Al1, Al2) and 4 Cu (Cu1 to Cu4) samples were machined to the desired shape. They were then hand-polished using sequentially abrasive papers P400, P800, P2500, P4000, and finally $1 \mu\text{m}$ diamond paste. A verification on a profilometer gives a roughness of $\approx 20 \text{ nm}$ on the surface with some scratches in the $100 - 500 \text{ nm}$ range. There are more and deeper scratches for Al, for which a homogeneous polishing is difficult to achieve since particles are easily detached from the bulk during polishing. After polishing, a first “soft” cleaning sequence has been applied: 3 minutes ultrasonic bath in RBS Neutral T – 6% concentration [40] – in hot water for Al and 3 minutes ultrasonic bath in RBS T 305 – 5% concentration [40] – in hot water for Cu, followed by 3 minutes ultrasonic rinsing bath in a beaker of hot water and 3 minutes ultrasonic bath in a beaker of ethanol, and finally drying with a soft cloth. The samples were then stored for days or weeks.

Immediately before Au evaporation or insertion of In, the samples underwent a stronger cleaning sequence:

- For Al and Cu: Remover (MicroChem 1112A [41]) ≈ 15 mins + Rinse with de-ionized water.
- For Al and Cu: Acetone 10 mins in ultrasonic bath + isopropyl alcohol 2 mins ultrasonic bath.
- For Al only: a standard ”Aluminium Etch” process as follows: 75% H_3PO_4 + 2-5% HNO_3 + 20% de-ionized water ≈ 12 mins + rinse in de-ionized water until resistance of water is $> 12 \text{ M}\Omega$. Note that the etching rate is expected to be around 20 nm/min resulting in the removal of up to $\approx 240 \text{ nm}$ of Al_2O_3 . After this step, the surface was slightly less mirror-like and surface pitting was visible in some places.

Setup with gold plating – sample reference Al1 + Cu3 (AB side) + Cu4 (CD side):

- About 40 minutes after cleaning, introduction of the 2 Cu pieces and Al block into an electron beam evaporator (Plassys model MEB550).
- Argon plasma etch with the following parameters: $I = 52 \text{ mA}$, $V = 600 \text{ V}$, 3 minutes with the samples under rotation (5 rpm)²
- Electron beam evaporation of 200 nm of Au with the following parameters: 0.5 nm/s deposit ($V = 9.85 \text{ kV}$, $I = 308 \text{ mA}$, 5 rpm rotation, vacuum level $\approx 2 \times 10^{-5} \text{ Pa}$).

² Very rough estimates based on measured etching rates of 7.4 nm/min for SiO_2 on Si and on [34] suggest an etching rate of $\approx 1.5 \text{ nm/min}$ for Al_2O_3 .

- Immediately after removal from the evaporator, the two gold surfaces were placed in contact. Compressive force was applied by alternately tightening the bolts.
- Application of an effort of 11 kN with a hydraulic press (performed 2 days after sample assembly).
- Re-tighten bolts to obtain a compression force of about 3 kN per bolt (5 Nm measured torque).

Setup with indium – sample reference Al2 + Cu1 (AB side) + Cu2 (CD side):

- A 99.999% purity piece of indium [42] approximately $1\text{ mm} \times 1\text{ mm} \times 15\text{ mm}$ was placed at the centre of the contact surface between the Al and Cu, which were then pressed together. A small sphere of indium was squeezed rather than a thin foil to limit the initial surface to volume ratio of the indium and consequently the quantity of oxide present on its surface.
- Assembly of Al + Cu parts in the clamp and tightening of the bolts progressively to 8.5 Nm. The applied force was insufficient to fully squash the indium.
- Application of an effort of 11 kN with a hydraulic press (performed 2 days after sample assembly).
- Re-tighten bolts to obtain compression of the Belleville washers of $\approx 0.7\text{ mm}$ (3 kN per bolt) – typical tightening torque 3.5 - 4.5 Nm

6 Results

Measurements are of 4 wire type. The two samples are mounted in series as presented in Fig. 7. The voltage is measured across each of the contact resistances (V1, V3, V4 and V5). Actually, for each of these measurements, there is a contribution from bulk Cu and Al. From their measured RRRs, we evaluate their total contribution to be about 3 n Ω for each of the two samples. Measurement V6 is used as a verification of the overall setup since the characteristics of the Al block are well known.

We used a program developed under LabViewTM to analyse the resistance of our samples. Each measurement sequence is achieved in several steps with current reversal between steps so as to compensate for thermo-electric effects. Each step lasts about 2 minutes and we programmed between 7 and 21 steps. The current (Kikusui Model PBZ40-10 current source) is chosen between 1 and 10 A. Copper current leads of low resistance run inside the cryostat and the current is injected into the samples at the level of the stainless steel support central screw (see Fig. 5). We always tested several current values in order to maximise the signal while checking for overheating effects. For each current step, voltages are measured sequentially using a Keithley model 2000 multi-meter equipped with a multiplexer. For each channel, the voltage is averaged over about 20 measurements during each current step. The corresponding resistance is averaged over the current steps, ignoring the first and second steps, during which the system is stabilizing.

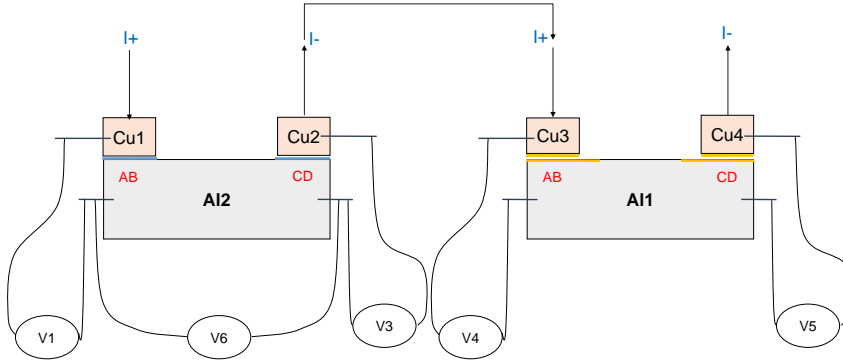


Fig. 7 Current and voltage pickups for the two samples (mounted in series). Left: with In filler (blue). Right: with Au deposit on Cu and Al (yellow).

We always made a first set of measurements at 300 K so as to check all the connections, verify the overall measurement chain, compare with the calculated value for bulk Al and get first results on the contact resistances. The samples are then slowly cooled down to 4.2K during several hours using first liquid nitrogen and then liquid helium.

Results obtained with these 2 samples (\Leftrightarrow 4 contacts) are summarized in Table 2. Prior to the second measurement sequence at 4.2 K, the bolts A & B on each sample (Cu1 & Cu3) were loosened by approximately 0.4 mm corresponding to a final force of ≈ 1.3 kN for each bolt. The measurements were repeated 4 months later. Finally, the bolts A & B on each sample were loosened to 0.2 mm compression of Belleville washers corresponding to a final force of ≈ 0.87 kN for each bolt. For this latest cool down, we also removed Belleville washers on bolts C & D on each setup (Cu2 & Cu4) then tightened back the bolts to 0.75 Nm, which corresponds to a force between 0.7 to 1 kN (friction coefficients between 0.18 and 0.12) for each bolt. We chose such low forces and also to remove Belleville washers in order to mimic the most simple cryogenic setup one can think of.

Whatever the type of junction, gold plated or with indium filler, the resistances at 4.2 K are close to or below 20 n Ω . The best results are obtained with gold plating. For the 2 gold plated samples, resistances cannot be distinguished from the expected contribution of bulk materials. Furthermore, no degradation with time is observed and there seems to be no dependence on the applied force, at least down to our minimum ≈ 1.5 kN total force. The 11 kN force applied with the press may have "frozen" the Al-Au-Cu interfaces so that it is not necessary to maintain a strong force on the contact area.

Table 2 Synthesis of resistance measurements.

Contact Ref.	R (300 K) nΩ	R (4.2 K) nΩ	RRR	R (4.2 K) nΩ	R (4.2 K) nΩ	R (4.2 K) nΩ
	28/11/19	29/11/19		14/01/20	20/05/20	29/05/20
Cu3-Au-Al1	274±73	3±6	91	4±3*	3.6±4	3.1±3 [†]
Cu4-Au-Al1	297±62	2±7	149	4±4	3.2±3	4.7±3 [•]
Cu1-In-Al2	715±63	12±8	60	14±3*	24±6	23.4±5 [†]
Cu2-In-Al2	672±67	8±7	84	10±3	13±6	16±5 [•]

* Bolts loosened by about 0.4 mm

[†] Bolts loosened to 0.2 mm compression of Belleville washers

[•] Belleville washers removed and bolt tightened back to 0.75 Nm

The contact resistances are higher with indium. They do not seem to depend much on the applied force either, but may degrade with time. This latter effect is difficult to quantify due to measurement uncertainties.

7 Complementary results and discussion

In this section, we give complementary information deduced from previous measurements (with few details for clarity purpose):

- It has been suggested [24,35] that highly polished surfaces usually don't give the lowest resistances. But, on the other hand, evaporated gold is expected to adhere better to a highly polished surface. We have tested roughly polished gold plated samples (typ. 1 μm roughness for Al and Cu) but in all cases the resistance was above 100 nΩ, even after addition of indium as a filler. We cannot confirm that polishing in the 20-40 nm range is an optimum but rough samples do not give very low resistances.
- For a sample undergoing a less aggressive argon etching (≈ 2.5 times less Al₂O₃ removed compared to previous sample) and experiencing a lower force (≈ 6 kN via screwing instead 11 kN via hydraulic press), the contact resistance was above 230 nΩ initially and degraded with time. We believe this to be caused by residual Al₂O₃ which could then serve as starting point for further oxidation. Application of 8 kN via hydraulic press on a similar sample only reduced the resistance from 240 nΩ to 140 nΩ.
- We dismounted some of the samples for visual inspection. The force required to separate the polished and gold plated copper and aluminium pieces was not negligible (but still by hand). All the gold over the contact area had transferred to the copper block, leaving a bare aluminium surface. Note that in the case of the roughly polished sample, the parts separated spontaneously which suggests that a more intimate contact is obtained for highly polished surfaces.

8 Conclusion

We have demonstrated that very low Al/Cu contact resistances at low temperature – in the order of a few $\text{n}\Omega$ – can be achieved with rather simple methods: one with the use of an indium filler (and no gold plating) and one with gold plating in a standard evaporator for micro-electronics. The gold plating samples gave better results and seem to be more stable with time.

Furthermore, unlike indium, gold will not undergo any superconducting transition at low temperature, which might affect the thermal conductance of the joint.

The necessary elements for obtaining such low Al/Cu contact resistances seem to be:

- A fine polishing of the Al and Cu surfaces.
- The total removal of the Al_2O_3 oxide layers. These layers are partially removed by chemical etching. For gold plated samples, complete removal is achieved via an Ar etching followed by Au evaporation without air exposure in between. For samples using indium, we believe that friction between the aluminum and the indium when the latter is squashed between the smooth surfaces is sufficient to break the oxide layer.
- The application of strong compression forces, but only temporarily.

We believe these contacts are not compatible with multiple disconnections. It is obvious for samples using indium since, after dismounting, we saw that the Al block was strongly imprinted. For the gold plated samples, the gold will probably remain stuck to the copper piece, thus allowing the aluminium surface to oxidize again.

It might be interesting to measure the thermal conductance of the Al/Cu contacts at low temperatures. First, this would provide further information on the applicability of the Wiedemann-Franz law for contacts at low temperature since there are conflicting results in the literature. On one side a discrepancy up to a factor of 2.5 has been reported [36] while discrepancies are much smaller for Gloos et al. [16] – see Table 1. This would also allow testing the effect of the indium filler far below its superconducting transition. For the purpose of the construction of the CNDR, similar tests with (Cu-Au)-(Au-Cu) contacts will be needed in order to keep the overall heat switch dismountable together with a resistance below the required value of $150 \text{ n}\Omega$.

Acknowledgements We acknowledge support from the ERC StG grant UNIGLASS No.714692 and ERC CoG grant ULT-NEMS No. 647917. The research leading to these results has received funding from the European Union’s Horizon 2020 Research and Innovation Programme, under Grant Agreement no 824109.

This work has been performed at the “Plateforme Technologique Amont” (PTA) of Grenoble.

Appendix

Table 3 Some of the lowest published (sorted by publication date) Cu-Cu or Cu-Al contact resistances at low temperature.

Ref.	Assy.	Technology	Variable	Published Value	Equiv. Res.	Est. force*	Comments
[11]	Cu-Al	Al foils pressed against Cu foils + gold plating (zincate solution for Al) with 3×M3 brass screws nearly to the tension at which they yield	Conductance	21 μWmK^{-1} at 66 mK	77 n Ω	2.7 kN	Measured at 66 mK
[27]	Cu-Cu	2 Cu blocks (10 mm diameter), NC8-32 SS screw. 4 Nm.	Electrical R.	57 n Ω	57 n Ω	≈ 3 kN	Measured at 4.2 K
[27]	Cu-Cu	Same as above + indium filler	Electrical R.	5 n Ω	5 n Ω	≈ 3 kN	Same as above
[29]	Cu-Cu	2 gold plated copper disks (4 mm thick) pressed with SS bolt. No filler. 4 Nm	Electrical R.	10 n Ω	10 n Ω	5.3 kN	Measured at 4.2 K. Current decay method.
[29]	Cu-Cu	Same as above + indium filler. 5 Nm	Electrical R.	4 n Ω	4 n Ω	6.6 kN	Same as above
[30]	Cu-Al	Cu (1 mm) - Al (0.5 mm) - Cu (1 mm) plates impact welded + etched Cu	Thermal R.	1.3/T KW^{-1}	32 n Ω		From 27 mK to 250 mK
[28]	Cu-Al	Al foil (0.1 mm) pressed onto Cu block. Use of a zincate solution (bondar dip) for Al	Electrical R.	5 n Ωcm^{-2}			Measured at 4.2 K

* Extracting a force from the applied torque seems not a trivial procedure. For example, Deutsch [27] reports a torque of 4 Nm with a NC8-32 SS screw. The corresponding force may vary by more than a factor of 4 depending on the actual input parameters. First, there are various expressions for the calculation of the force and some might be erroneous. As an example, if one assumes that the parameter D from equation (8) provided in [21] is equivalent to the parameter $0.5 \times (d_s + d_h)$ from equation (A1) in [26], then the pre-factor for this contribution differs by a factor of 2. We believe [26] should preferably be considered. But, mainly, there is a large dispersion in the friction coefficients to be used in these equations. In [21], a friction coefficient of 0.12 is assumed while it is of 0.53 in [26]. From our understanding, the first one is better adapted to SS-SS bolts while the second one corresponds to a dry SS-Cu connection. In reference [55] of Dhuley's article, we also find that the friction coefficient for SS-304L to Cu would be of 0.23 in the worst case. Taking equation (A1) from Dhuley together with his parameters for UNC 8-32 screws (table 2 in [26]), and a torque of 4 Nm one can calculate forces of 1.4 kN, 3 kN and 5.4 kN for $\mu = \mu_b = 0.12, 0.23$ and 0.53 respectively. We believe $\mu = 0.23$ is more realistic and we thus propose 3 kN equivalent force in the table.

References

1. G. Pickett, C. Enss, *Nature Reviews Materials* **3**(3), 1 (2018)
2. I. Todoshchenko, J.P. Kaikkonen, R. Blaauwgeers, P.J. Hakonen, A. Savin, *Review of Scientific Instruments* **85**(8), 085106 (2014)
3. G. Batey, A. Casey, M. Cuthbert, A. Matthews, J. Saunders, A. Shibahara, *New Journal of Physics* **15**(11), 113034 (2013)
4. F. Pobell, *Matter and methods at low temperatures*, vol. 2 (Springer, 2007)
5. S. Riabzev, A. Veprik, H. Vilenchik, N. Pundak, *Cryogenics* **49**(1), 1 (2009)
6. D. Schmoranzler, A. Luck, E. Collin, A. Fefferman, *Cryogenics* **98**, 102 (2019)
7. R. Toda, S. Murakawa, H. Fukuyama, in *J. Phys. Conf. Ser.*, vol. 969 (2018), vol. 969, p. 012093
8. D. Schmoranzler, R. Gazizulin, S. Triqueneaux, E. Collin, A. Fefferman, *Journal of Low Temperature Physics* **196**(1-2), 261 (2019)
9. P. Shirron, E. Canavan, M. DiPirro, J. Francis, M. Jackson, J. Tuttle, T. King, M. Grabowski, *Cryogenics* **44**(6-8), 581 (2004)
10. D. Schmoranzler, J. Butterworth, S. Triqueneaux, E. Collin, A. Fefferman, *Cryogenics* **110**, 103119 (2020)
11. R. Mueller, C. Buchal, T. Oversluiszen, F. Pobell, *Review of Scientific Instruments* **49**(4), 515 (1978)
12. K. Gloos, C. Mitschka, F. Pobell, P. Smeibidl, *Cryogenics* **30**(1), 14 (1990)
13. M. Krusius, D. Paulson, J. Wheatley. Superconducting switch for large heat flow below 50 mk (1978)
14. N.S. Lawson, *Cryogenics* **22**(12), 667 (1982)
15. E. Schuberth, *Review of Scientific Instruments* **55**(9), 1486 (1984)
16. K. Gloos, P. Smeibidl, C. Kennedy, A. Singsaas, P. Sekowski, R. Mueller, F. Pobell, *Journal of low temperature physics* **73**(1-2), 101 (1988)
17. Y.M. Bunkov, *Cryogenics* **29**(9), 938 (1989)
18. P.C. Ho, R. Hallock, *Journal of low temperature physics* **121**(5-6), 797 (2000)
19. W. Yao, T. Knuuttila, K. Nummila, J. Martikainen, A. Oja, O. Lounasmaa, *Journal of low temperature physics* **120**(1-2), 121 (2000)
20. T. Tajima, R. Masutomi, A. Yamaguchi, H. Ishimoto, *Physica B: Condensed Matter* **329**, 1647 (2003)
21. F. Blondelle, A. Sultan, E. Collin, H. Godfrin, *Journal of Low Temperature Physics* **175**(5-6), 877 (2014)
22. R. Schmitt, G. Tatkowski, M. Ruschman, S. Golwala, N. Kellaris, M. Daal, J. Hall, E.W. Hoppe, *Cryogenics* **70**, 41 (2015)
23. I. Didschuns, A. Woodcraft, D. Bintley, P. Hargrave, *Cryogenics* **44**(5), 293 (2004)
24. L.J. Salerno, P. Kittel, (1997)
25. E. Gmelin, M. Asen-Palmer, M. Reuther, R. Villar, *Journal of Physics D: Applied Physics* **32**(6), R19 (1999) + Comment by A. L. Woodcraft, *J. Phys. D: Appl. Phys.* **34**, 2932 (2001)
26. R. Dhuley, *Cryogenics* **101**, 111 (2019)
27. M. Deutsch, *Cryogenics* **19**(5), 273 (1979)
28. T. Shigematsu, M. Maeda, M. Takeshita, Y. Fujii, M. Nakamura, M. Yamaguchi, T. Shigi, H. Ishii, in *Proceedings of the Sixteenth International Cryogenic Engineering Conference/International Cryogenic Materials Conference* (Elsevier, 1997), pp. 621–624
29. T. Okamoto, H. Fukuyama, H. Ishimoto, S. Ogawa, *Review of scientific instruments* **61**(4), 1332 (1990)
30. R. Willekers, W. Bosch, F. Mathu, H. Meijer, H. Postma, *Cryogenics* **29**(9), 904 (1989)
31. M. Wanner, *Cryogenics* **21**(1), 3 (1981)
32. R. Raoulison, D. Racine, Z. Zhang, N. Buiron, D. Marceau, M. Rachik, *Journal of Manufacturing Processes* **16**(4), 427 (2014)
33. J. Goupy, A. Benoit, A. Bidaud, O. Bourrion, M. Calvo, A. Catalano, E. Driessen, A. Gomez, S. Leclercq, F. Levy-Bertrand, et al., *Journal of Low Temperature Physics* **193**(5-6), 739 (2018)
34. <http://apps.mnc.umn.edu/pub/pdf/equipment/ionmill.rates.pdf>

-
35. D. Guillaume, Etude bibliographique des résistances thermiques de contact, Note SBT/CT/90-38, CEA – CENG
 36. R. Boughton, N. Brubaker, R. Sarwinski, Review of Scientific Instruments **38**(8), 1177 (1967)
 37. Alfa Aesar, ref. 44551
 38. Alfa Aesar, ref. 44336
 39. Laurand Associates, Inc
 40. <http://www.rbs-cp.be/documents/cp-anglais/brochures/LABCP301ABR100217.pdf>
 41. <https://kayakuam.com/wp-content/uploads/2019/09/MicroChem-Remover-1112A-v07.15.pdf>
 42. Advent Research Materials catalogue #IN159701